Modeling of Strain in Boron-Doped Silicon Cantilevers

Hernan A. Rueda and Mark E. Law

Department of Electrical and Computer Engineering, University of Florida
Gainesville, FL 32608-6200 USA
har@tec.ufl.edu law@tec.ufl.edu

ABSTRACT

A finite element method is developed to compute the mechanical strain resulting from boron doping in silicon. This technique is then applied to the bending of boron-doped silicon cantilevers. The silicon cantilever is modeled as an isotropic elastic material. A lattice mismatch parameter due to the substitutional boron is used as the strain source. Qualitative agreement is resulted with experiments in the literature for varying thickness cantilevers.

Keywords: finite element method, boron, strain, cantilevers, residual stress

INTRODUCTION

Silicon bulk micromachining is important for fabricating silicon-based sensors and transducers. Silicon sensors are often composed of thin membranes, bridges, cantilevers, and beams. These structures can be fabricated by various bulk micromachining methods. Anisotropic wet chemical etching is often used to develop sensor structures due to its simplicity and convenience as well as providing very accurate dimensional control [1].

Boron etch stops are often used as a method for controlling etch depth in silicon substrates. Thin silicon film structures can be fabricated by thermally diffusing or implanting boron on one surface of the silicon wafer and then by etching through a mask window on the other side of the wafer. For wet chemical etchants such as KOH, the etch rate decreases significantly as the etch front approaches boron concentrations greater than 7×10^{19} cm^{-3}. It is believed that the strong B-Si bond tends to bind the crystal more stringently, therefore requiring more energy to release the silicon atom [2].

It is then possible to design thin silicon film structures with the desired thickness by controlling the diffusion of the boron dopant profile so that the etch stop will occur at depth where the boron concentration approaches $\sim7\times10^{19}$ cm^{-3}. However due to these levels of boron concentration, high levels of residual stress are generated. Since micromachined thin membranes are critical components of silicon sensors and transducers, residual stresses in these structures may lead to mechanical failure of the device and/or deteriorate its performance.

It is well known that boron is a substitutional dopant in silicon and exerts a tensile strain when introduced into the crystal lattice [3]. As the smaller boron atom displaces the silicon atom, there is a tendency for the lattice to contract locally. However, the silicon lattice will restrain from contracting and therefore result in a local tensile strain, as is demonstrated in Figure 1.

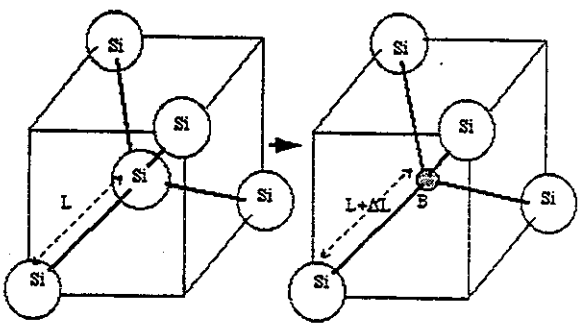

Figure 1. A local tensile strain is generated as a boron atom substitutes into a silicon lattice site.

The high concentrations of boron necessary to produce the etch stop behavior results in residual tensile stress with magnitudes approaching and exceeding levels of 1×10^{9} dyn/cm^2. To relieve these high levels of stress the silicon crystal yields and may generate dislocations that may be deleterious to device and sensor performance [4]. This is one of the main reasons for studying residual stress and its origins.

The residual stress resulting is dependent on the gradient and maximum magnitude of the boron dopant profile as well as the thickness of the cantilever resulting after the backside etch. Since the boron dopant profile is not uniform the stress distribution varies with depth causing the cantilever to bend in order to relieve the resulting residual stress. This is evident in previous studies analyzing positive and negative bending of boron-doped cantilevers under varying diffusion conditions [5, 6].

This paper presents a finite element based model that computes the residual stress field resulting from a particular boron diffusion process and its corresponding cantilever bending behavior.

FEM FORMULATION

The process simulator FLOOPS [7] has been implemented to study and analyze the residual stress due to the boron dopant. A finite element method has been developed to compute the stress resulted from the boron layer along with other sources of stress in microelectronics technology [8]. This framework has then been adapted here to model the residual stress in micromachined structures.

Equivalent Nodal Forces

From the theory of equivalent nodal forces and virtual work [9], the equivalent elemental force q^e can be described by the following relation:

$$q^e = \int_{V^e} B^T \sigma d(vol) - f_b^e \tag{1}$$

where B^T is the transpose of the vector relating the strain to nodal displacements, f_b represents element's distributed body forces, and σ is the stress tensor. Since Equation 1 is derived for any virtual displacement, it can be used in conjunction with any stress-strain relationship.

For a linear elastic solid such as silicon, the following relationship between stress and strain is known as Hooke's law:

$$\sigma = D(\varepsilon - \varepsilon_0) + \sigma_0 \tag{2}$$

where D is the tensor of elastic constants and ε_0 and σ_0 are the initial strain and stress tensors respectively [10]. Substituting Hooke's law for the stress tensor, Equation 1 now becomes the following:

$$q^e = \int_{V^e} B^T D\varepsilon^e d(vol) - \int_{V^e} B^T D\varepsilon_0^e d(vol) + \int_{V^e} B^T D\sigma_0^e d(vol) - f_b^e \tag{3}$$

The B matrix relates the strain tensor ε to the nodal displacements a^e:

$$\varepsilon^e = Ba^e . \tag{4}$$

Solving for the nodal displacements in Equation 3 under mechanical equilibrium ($q^e = 0$) in the case of no initial strain or stress, yields the following simplified elastic relationship integrated over the volume of the element:

$$\int_{V^e} B^T DBa^e d(vol) = f_b^e \tag{5}$$

or in discretized form:

$$B^T DB\Delta a^e = f_b^e \tag{6}$$

where Δ is the volume of the element.

The isotropic approximation is used to simplify the tensor of elastic constants D. Therefore the silicon cantilever is modeled as an isotropic elastic material. The two-dimensional plane strain approximation is implemented to further simplify the computation. This assumption is valid for structures with infinite width in the z-direction where $\varepsilon_{zz} = \varepsilon_{yz} = \varepsilon_{zx} = 0$. A rigid boundary condition ($a_x = a_y = a_z = 0$) is imposed on the interface where the cantilever is attached to the substrate. Linear shape functions are utilized for interpolation of the strain solution within each element. Triangular elements are used for the 2D FEM implementation and tetrahedral elements constitute the 3D structures

Boron Strain-induced Body Forces

The force due to the boron dopant is modeled as a distributed body force and is assigned to the right hand side of Equation 6 for each element. The force is calculated through an average element strain mismatch parameter ε_B, similarly as if it were an initial strain:

$$f_b^e = \int_{V^e} B^T D\varepsilon_B^e d(vol) . \tag{7}$$

After integrating over the volume of the element, the following discretized form results:

$$f_b^e = B^T D\varepsilon_B^e \Delta . \tag{8}$$

The average element strain parameter ε_B is modeled by the following relationship:

$$\varepsilon_B^e = \frac{\delta_B}{A_{Si}} \cdot \frac{C_{Boron}^{e*}}{C_{Si}}(100) \tag{9}$$

Through densitometric studies, F. Horn reported that the boron induced lattice contraction is linearly proportional to the atomic percentage of boron in silicon [3]. Extracting from Horn's measurements, it is found that the silicon crystal lattice contracts at 0.014 Å per atomic % boron. This constant is used as the lattice contraction parameter δ_B in Equation 9. Since the boron concentration is a nodal quantity, the average element boron concentration is computed from its nodes' concentrations. This average concentration is divided by the atomic density of silicon ($C_{Si} = 5\times10^{22}cm^{-3}$) for estimation of the local elemental atomic percentage of boron. The lattice displacement is then the product of atomic percentage and δ_B. The local boron-induced strain is then computed by dividing this lattice displacement result by the equilibrium lattice constant of silicon ($A_{Si} = 5.4295$ Å).

ANALYSIS

The method previously described is now applied for

studying the strain-induced bending of boron-doped cantilevers. The cantilever bending behavior is then studied after regridding the deformation of the structure according to the displacement solution.

As was noted previously, the bending of the cantilever is dependent on the boron concentration, its concentration gradient, its position with respect to the center of the cantilever, and the cantilever thickness. A uniform profile of boron dopant (Figure 2a) does not cause bending due to the entire thickness of the cantilever being subjected to an equal amount of tensile boron-induced stress. No bending also occurs if the boron profile is symmetrical about the center axis of the cantilever (Figure 2b).

Cantilevers with dopant profiles more heavily doped on one side of the center and having a sharp gradient will induce deflection in the direction away from the more highly doped side (Figure 3). Cantilevers that are products of the boron etch stop process usually have the characteristics of the more heavily doped side towards the substrate as in Figure 3a. This is due to the high boron concentration required for the etch stop on the backside. Thinner cantilevers produce greater deflections than ones with thicker dimensions having the same dopant profile due to less moment of inertia.

APPLICATION

Simulations are performed using the finite element models previously described for the cantilever process described in Figure 4. First boron is introduced by thermal diffusion. The resulting profile has a peak concentration of 8×10^{19} cm^{-3} (Figure 5). A backside wet chemical etch is then performed. A boron concentration of 6×10^{19} cm^{-3} is chosen as the stop for this etch. The resulting cantilever

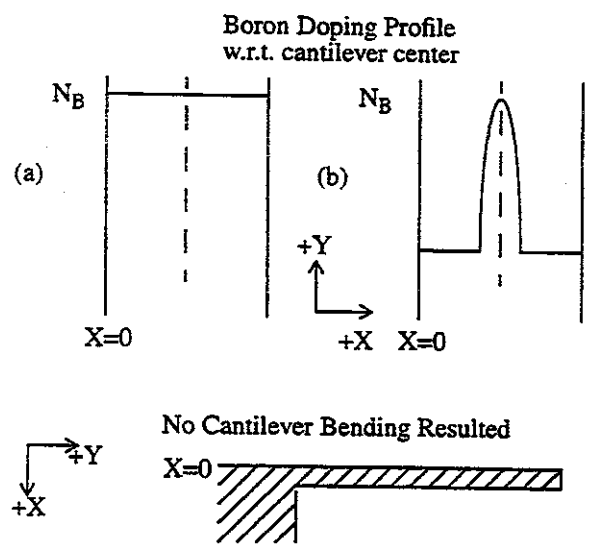

Figure 2. A uniform boron profile (a) or a boron profile that is symmetric about the cantilever center (b) does not induce cantilever bending.

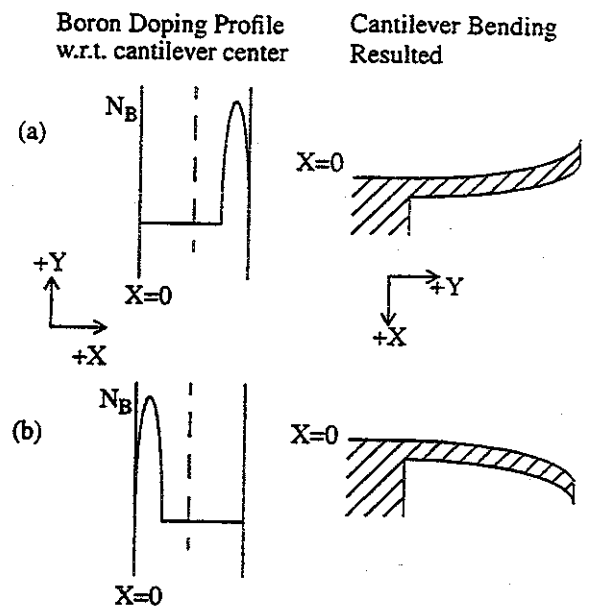

Figure 3. The tensile strain induced by the boron dopant causes the cantilever to curl away from the more region highly doped region.

thickness is about 1.4 μm.

Next a series of 2d plane strain and 3d elastic deformation simulations is performed for the resulting boron-doped cantilever structures. The 2d cantilever has a length of 50 μm. The grid spacing in the x-direction is 0.05 μm and in the y-direction is 0.5 μm. Since the x-direction spacing is limited by the necessary resolution to represent the boron profile, it becomes a challenge to preserve element quality as the cantilever length is increased while maintaining the number of elements constant. The element aspect ratio problem is magnified further in three dimensions. The 3d cantilever

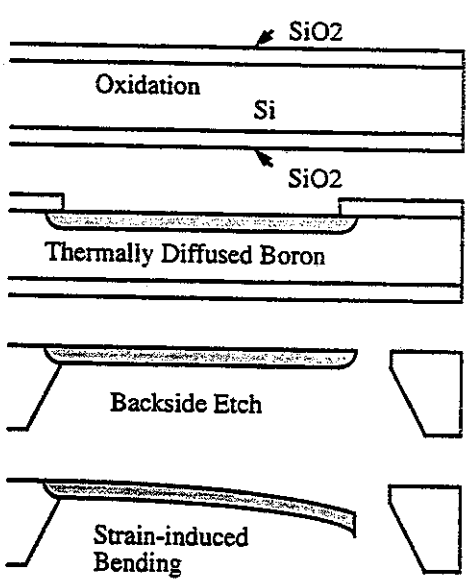

Figure 4. Process flow for fabrication of the cantilever.

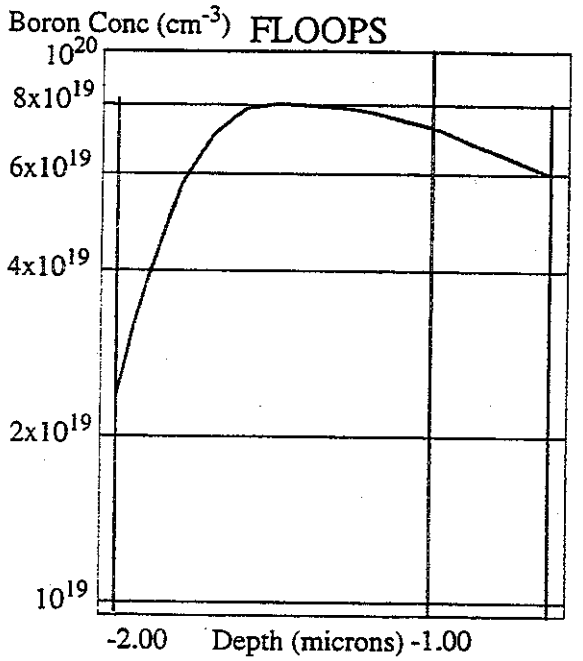

Figure 5. Resulting cantilever boron profile with a thickness of 1.4 μm.

has dimensions of 1 μm width and 10 μm length. The 3d cantilever grid spacing is 0.3 μm in the z-direction (width), 0.5 μm in the y-direction (length), and 0.1 μm in the x-direction (thickness).

The following mechanical material properties were utilized for all simulations performed: Young's modulus (E_{p+Si} = 1.22×10^{12} dyn/cm^2) [11], Poisson's ratio ($\upsilon = 0.3$).

A series of varying front side etch simulations were performed to analyze how the shift in boron profile and decrease in thickness of the cantilever affected the deflection solution. These series of etch simulations model the experiment performed by Yang [6].

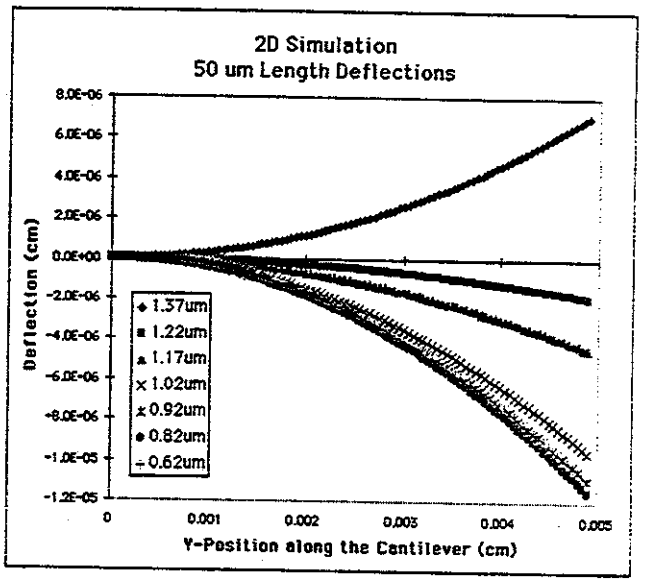

Figure 6. Deflection curves for different thickness cantilevers simulated by 2d plane strain elastic FEM.

RESULTS

The results of the 2d plane strain simulations are displayed in Figure 6. An example of the deflection simulation for the 0.62 μm thickness beam is shown in Figure 7. The structure is regridded after the nodal displacements are solved for. Figure 6 displays the nodal displacements along the top surface of each cantilever structure simulated. The differences between each structure thickness relates to the amount etched off the top surface. Notice that all the cantilever beams except the thickest deflected in the negative x-direction (upward in Figure 7). Generally as the cantilevers were etched thinner, the amount of deflection increased.

A 3d simulation for the 1.37 μm thickness cantilever is demonstrated in Figure 8. It is more difficult to examine the deflection visually in the 3d simulations due to the shorter

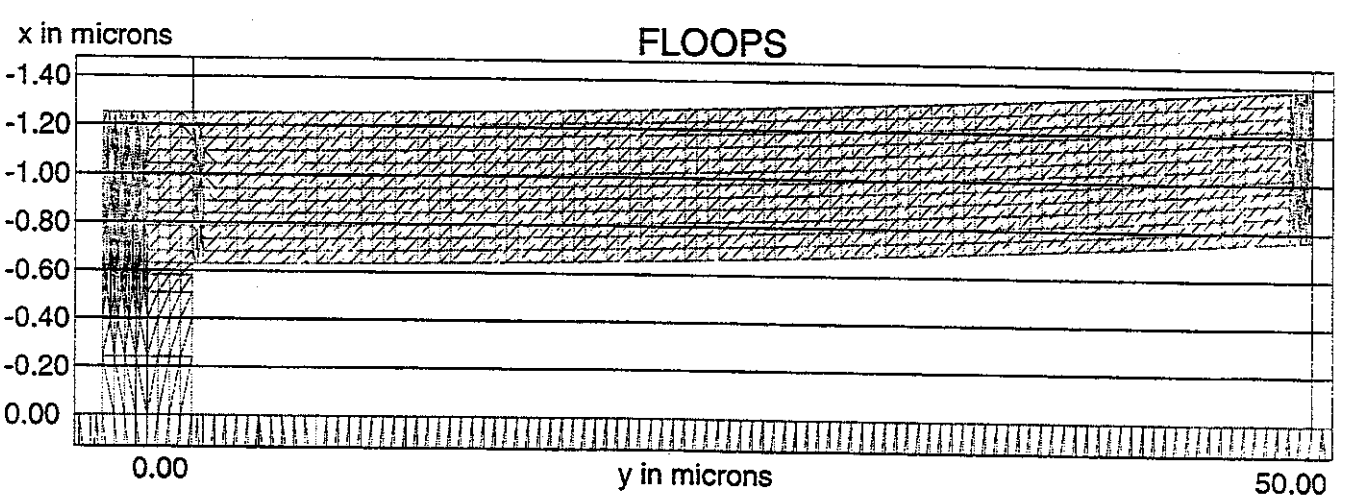

Figure 7. Two-dimensional plane strain simulation of the deflection of a 0.6 μm thickness cantilever.

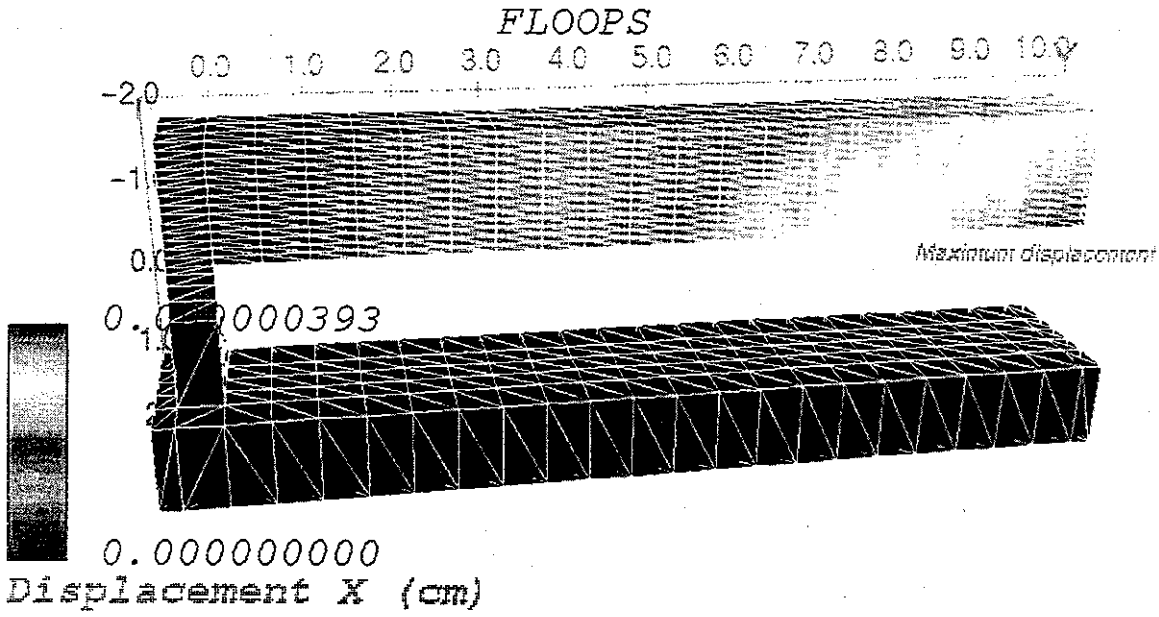

Figure 8. Three-dimensional simulation of the deflection of a 1.37 μm thickness cantilever. The maximum deflection resulted is observed to be at the bottom corner tip of the cantilever beam.

length of the cantilevers. The deflection solution plot for the 3d simulations is displayed in Figure 9. The same general trend also results.

The simulation lengths of the cantilever beams are much shorter than the those fabricated in various experiments [5,6]. Typically cantilever beams are fabricated with lengths up to 1mm in order to have an accurate measurement of the deflection. The element quality problem limits the length of the cantilevers simulated before a significant error is resulted in the elastic solution.

To compare the simulations performed with experiments in the literature, a parabolic curve fit was used to extrapolate the expected deflections for longer cantilever beams. This is possible because beams processed the same with varying lengths would all have the same bending moment [5]. This is illustrated in Figure 10.

Therefore, the cantilever deflection simulation results are then extrapolated to amounts corresponding to 1250 μm to compare with experiments performed by Yang [6]. These results are presented in the histogram shown in Figure 11. Several points can be deduced from the results obtained. First is the 2d and 3d simulations resulted in roughly the

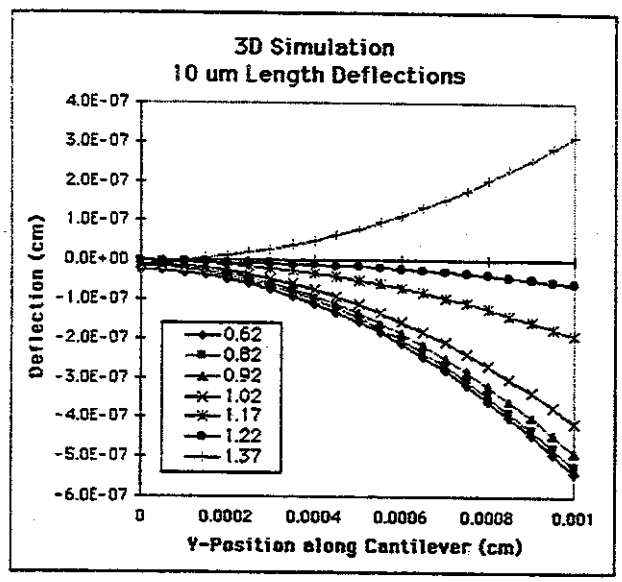

Figure 9. Deflection curves for different thickness cantilevers simulated by 2d elastic FEM.

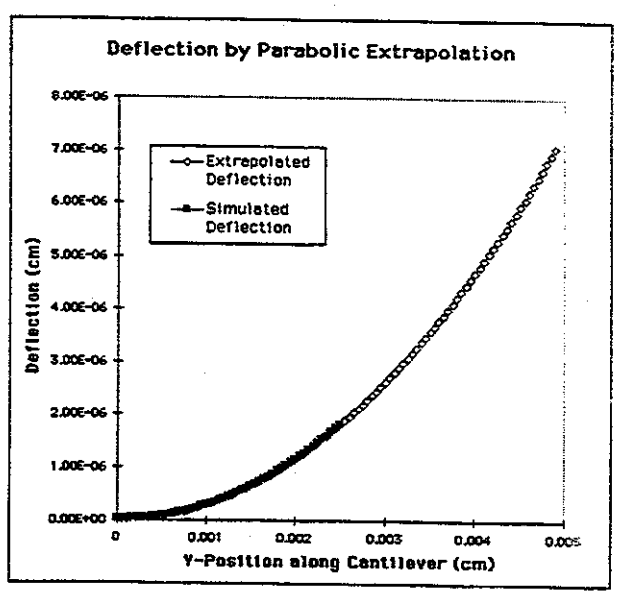

Figure 10. Longer cantilever deflection solutions are extrapolated by parabolic curve fits.

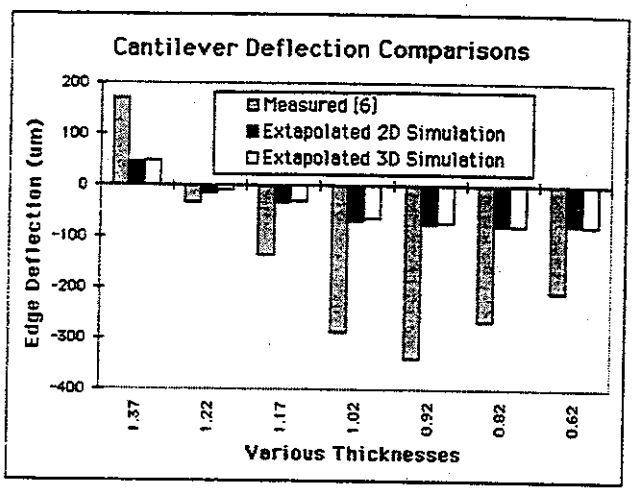

Figure 11. Results of both sets of simulations compared with Yang experiment [6].

same amount of deflection. This confirms that the plane strain approximation does not affect the result of the simulation and that cantilever width is not a factor in the stress solution. Second, both the simulations agree with the published experiment in the direction of the deflection for each beam thickness. However the measured deflection results are consistently about two to three times the magnitude of the simulations. Also the measured quantities have a relative maximum negative deflection for the 0.92 μm thick beams, while the simulations showed relatively constant deflections for cantilevers of less thickness.

CONCLUSION

The observation that the simulations agreed qualitatively with the measured experiment is encouraging. There were differences in the relative maximums as well as the magnitude of deflection. It is believed that the relative negative maximum difference is attributed to differences in the simulated boron profile, either in concentration magnitude and/or in a shift in depth.

The difference in deflection magnitudes is attributed to the lattice contraction parameter used for the boron-induced strain model. By simply scaling this parameter, the simulation deflection magnitudes would coincide better with the measurements. This leads to believe that the lattice contraction parameter used for the boron induced strain model may need to be scaled for the case of thin film thickness. It may be that the boron-induced lattice contraction X-ray diffraction measurements may be different for diffused boron with a shallower depth as opposed to the bulk p^+-silicon wafer measurements that were performed [3]. The thickness of the deformed layer may need to be taken into account in scaling the lattice contraction. The FEM cantilever deflection solution may then give insight to the magnitudes of residual stress inherent in the cantilevers that is induced by boron dopant.

ACKNOWLEDGMENTS

The authors would like to thank Paul Colestock for help with the use of the Tonyplot3d and Silvaco for the use of Tonyplot3d software to render the three-dimensional cantilever simulations.

REFERENCES

[1] B. Kloeck and N. F. DeRooij, "Mechanical Sensors," in Semiconductor Sensors, S. M. Sze, Ed. New York, NY: John Wiley and Sons, Inc., 1994, pp. 153-204.

[2] K. E. Peterson, "Silicon as a mechanical material," Proceedings of the IEEE, vol. 70, pp. 420-457, 1982.

[3] F. H. Horn, "Densitometric and electrical investigation of boron in silicon," Physical Review, vol. 97, pp. 1521-1525, 1955.

[4] X. J. Ning, "Distribution of residual stresses in boron doped p+ silicon films," Journal of the Electrochemical Society, vol. 143, pp. 3389-3393, 1996.

[5] W.-H. Chu and M. Mehregany, "A study of residual stress distribution through the thickness of p+ silicon films," IEEE Transactions on Electron Devices, vol. 40, pp. 1245-1250, 1993.

[6] E. H. Yang and S. S. Yang, "The quantitative determination of the residual stress profile in oxidized p+ silicon films," Sensors and Actuators A: Physical, vol. 54, pp. 684-689, 1996.

[7] M. E. Law, "Florida Object-Oriented Process Simulator, FLOODS/FLOOPS Manual," University of Florida, Gainesville 1993.

[8] H. Rueda, S. Cea, and M. Law, "Mechanical stress modeling for silicon fabrication processes," presented at SISPAD 97, Cambridge, MA, 1997.

[9] O. C. Zienkiewicz and R. L. Taylor, The Finite Element Method, vol. 1, 4ed. London, U.K.: McGraw-Hill Book Company, 1987.

[10] Y. C. Fung, A First Course in Continuum Mechanics, 3 ed. Englewood Cliffs, N. J.: Prentice Hall, 1994.

[11] X. Ding, W. H. Ko, and J. M. Mansour, "Residual Stress and Mechanical Properties of Boron-doped p+ Silicon Films," Sensors and Actuators A: Physical, vol. 21-23, pp. 866-871.